Phase synchronization between task-positive and task-negative brain networks using Hilbert Huang Transform for Alzheimer's disease

Pavithran Pattiam Giriprakash[1], Filippo Cieri[1], Xiaowei Zhuang[1], Zhengshi Yang[1], Chendi Han[1], and Dietmar Cordes[1,2]
[1]Lou Ruvo Center for Brain Health, Cleveland Clinic, Las Vegas, NV, United States, [2]Institute of Cognitive Science, University of Colorado Boulder, Boulder, CO, United States

Synopsis

Motivation: Resting-state fMRI studies of brain network connectivity have primarily focused on linear, frequency-independent relationships.

Goal(s): The primary goal of this study is to quantify the synchronization between brain regions using instantaneous phase information and evaluate their relationship with amyloid deposition in the brain.

Approach: Empirical Mode Decomposition (EMD) is utilized to investigate differences in phase synchronization between task-positive and task-negative brain networks across amyloid positive cognitively normal (CN), mild cognitive impairment (MCI) and Alzheimer's disease (AD) patients.

Results: A decreased phase synchronization was observed in MCI and AD patients compared to CN. CN and MCI exhibited opposite relationships with amyloid deposition.

Impact: Phase synchronization via EMD offers brain connectivity analysis with higher temporal resolution and frequency specificity. It could track network disruptions during disease progression. It could also highlight the influence on amyloid deposition, revealing insights on pathophysiology mechanisms involved in AD.

Introduction

Previous studies have identified anticorrelations between task-positive and task negative resting state networks (RSNs) and were shown to be associated with abnormal levels of cerebrospinal fluid (CSF) based biomarkers in patients with mild cognitive impairment (MCI) and Alzheimer's disease (AD)[1,2]. However, functional connectivity is a linear measure and lacks frequency specific relationships. In contrast, phase synchronization provides higher temporal resolution and captures nonlinear relationships but is limited to narrowband signals[3,4]. In this study, we estimate frequency specific phase synchronization between task-positive and task-negative RSNs from Empirical Mode Decomposition (EMD)[5] derived intrinsic mode functions (IMFs) using the Hilbert transform (HT). The association between phase synchronization and brain amyloid deposition was then analyzed.

Methods

Data used for this study was obtained from the Alzheimer's Disease Neuroimaging Initiative (ADNI) database (adni.loni.usc.edu). Only amyloid-β positive subjects (^{18}F-florbetapir AV-45 PET standardized uptake value ratio[6], SUVR ≥ 1.1) were included in the analysis. A total of 292 functional magnetic resonance imaging (fMRI) sessions from 74 cognitively normal (CN) (36 Male; age: 75.4 ± 5.7 years; years of education: 16.6 ± 2.7), 119 MCI (56 Male; age: 73.6 ± 6.9 years; years of education: 15.6 ± 2.7) and 99 AD (47 Male; age: 75.7 ± 8.1 years; years of education: 15.1 ± 2.4) were included. The resting state fMRI were acquired with the following parameters (TR/TE/resolution = 3000ms/30ms/3.3x3.3x3.3mm^3, flip angle = 90º, slice thickness=3.4 mm, echo spacing=0.72 ms). Standard spatial preprocessing was followed with temporal preprocessing consisting of detrending and variance normalization. Group Independent Component Analysis (ICA) based on FastICA[7] with tanh nonlinearity was implemented on temporally concatenated timeseries from all three groups to obtain 30 independent components. Then, 4 components representative of task-positive (left and right frontoparietal networks, lFPN and rFPN) and task-negative RSNs specifically the anterior and posterior default mode networks (aDMN and pDMN) were shortlisted for subsequent analysis. Back-reconstruction was performed using GIG-ICA[8]. HT was then applied to obtain the analytic signal for IMFs whose frequency spanned between 0.01 Hz and the 0.16 Hz (Nyquist frequency, f_{NQ}). Then, instantaneous phase information was utilized to estimate the phase synchronization based on the corrected imaginary part of phase locking value (ciPLV)[9] between all possible pairs of task-positive and task-negative RSNs (Figure 2). Statistical analysis was performed using a one-way ANOVA to identify significant group differences in ciPLV across these comparisons. To delineate the association between phase synchronization and amyloid deposition, partial correlation was performed between ciPLV and SUVR while controlling for the effect of age, education, gender, and handedness.

Results

Figure 1(a) shows the chosen task-positive (lFPN, rFPN) and task-negative (aDMN, pDMN) RSNs. Results of EMD applied to pDMN timeseries of the CN group where $IMF_{1\text{-}4}$ whose frequency is between 0.01 Hz and f_{NQ} were shortlisted for subsequent Hilbert spectral analysis (Figure 1(b), 1(c)). A significantly reduced ciPLV was observed between aDMN and both left and right frontoparietal networks (lFPN, rFPN) across MCI and AD patients compared to CN (figure 3 and table 1). With respect to phase synchronization between pDMN and frontoparietal networks, only AD group showed significantly reduced ciPLV than CN. These differences were localized to higher order IMFs, specifically, IMF_3 (0.01-0.04 Hz) and IMF_4 (0.005-0.02 Hz). No significant differences in synchronization were identified between MCI and AD patients (Table 1). Partial correlation analysis revealed a positive relationship between AV45 SUVR and phase synchronization between lFPN and pDMN (r=0.29, p = 0.01). In comparison, anticorrelation was observed between rFPN and aDMN (r=-0.19, p=0.04) in MCI patients. No association between amyloid deposition and phase synchronization was identified in AD patients.

Discussion

Disrupted phase synchronization in MCI and AD patients indicates a reduced ability to switch between task-positive and task-negative networks at rest compared to CN. In MCI, higher amyloid deposition disrupts the connectivity between RSNs resulting in reduced synchronization. However, RSNs in CN patients are more resilient to increase in amyloid deposition and in response show increased synchronization.

Conclusion

We have demonstrated that an adaptive time frequency analysis technique based on EMD can identify disrupted phase synchronization between task-positive and task-negative RSNs in MCI and AD. We also identified an inverse relationship between phase synchronization and amyloid burden in CN and MCI.

Acknowledgements

This work was supported by the NIH grants, R01AG071566 and P20GM109025.

References

1. Weiler, M. et al. Intranetwork and internetwork connectivity in patients with Alzheimer disease and the association with cerebrospinal fluid biomarker levels. J. Psychiatry Neurosci. JPN 42, 366–377 (2017).
2. Hampson, M., Driesen, N., Roth, J. K., Gore, J. C. & Constable, R. T. Functional connectivity between task-positive and task-negative brain areas and its relation to working memory performance. Magn. Reson. Imaging 28, 1051–1057 (2010).
3. Glerean, E., Salmi, J., Lahnakoski, J. M., Jääskeläinen, I. P. & Sams, M. Functional magnetic resonance imaging phase synchronization as a measure of dynamic functional connectivity. Brain Connect. 2, 91–101 (2012).
4. Honari, H., Choe, A. S. & Lindquist, M. A. Evaluating phase synchronization methods in fMRI: A comparison study and new approaches. NeuroImage 228, 117704 (2021).
5. Huang, N. E. et al. The empirical mode decomposition and the Hilbert spectrum for nonlinear and non-stationary time series analysis. Proc. R. Soc. Lond. Ser. Math. Phys. Eng. Sci. 454, 903–995 (1998).
6. Landau, S. M. et al. Amyloid deposition, hypometabolism, and longitudinal cognitive decline. Ann. Neurol. 72, 578–586 (2012).
7. Hyvarinen, A. Fast and robust fixed-point algorithms for independent component analysis. IEEE Trans. Neural Netw. 10, 626–634 (1999).
8. Du, Y. & Fan, Y. Group information guided ICA for fMRI data analysis. NeuroImage 69, 157–197 (2013).
9. Bruña, R., Maestú, F. & Pereda, E. Phase locking value revisited: teaching new tricks to an old dog. J. Neural Eng. 15, 056011 (2018).

Figures

Figure 1. (a) shows the thresholded spatial maps (z>2) for the chosen task-negative (aDMN, pDMN) and task-positive (lFPN, rFPN) RSNs from a group ICA with 30 components. Results of EMD of pDMN for the CN group shows the timeseries of the first 12 Intrinsic mode functions (IMF_i) in (b), and their corresponding frequency distributions in (c). Only the first 4 IMFs with $f_{drift} \leq f \leq f_{Nyquist}$ that have distributions to the right of the drift frequency are used for performing the group wise comparisons.

Figure 2. (a) shows the decomposition of a RSN time series using EMD into I IMFs and residual. The phase synchronization (ciPLV) for IMF i is calculated using instantaneous phase for two RSN time series according to (b). (c) shows instantaneous phases for RSNs aDMN and lFPN and the corresponding phase difference for IMF4 for a sample CN subject. N represents the length of the time series.

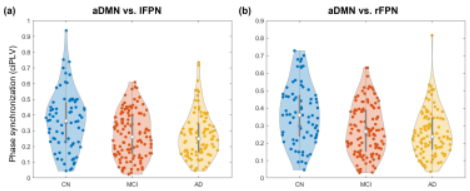

Figure 3. Distribution of the mean phase synchronization based on ciPLV across 3 groups (CN, MCI, and AD) are shown. ciPLV was estimated between a task-negative RSN (aDMN) and task-positive RSNs (lFPN and rFPN). For both cases (a) and (b), MCI and AD patients had reduced ciPLV compared to CN.

				Scheffe's post-hoc test					
RSN_1	RSN_2	IMF	p(Group)	CN vs. MCI		CN vs. AD		MCI vs. AD	
				Difference (95% CI)	p-value	Difference (95% CI)	p-value	Difference (95% CI)	p-value
rFPN	pDMN	2, 3	0.01, 1.8e-3	0.02 (-0.02,0.05), 0.04 (-0.01,0.08),	0.58, 0.13	0.05 (0.01,0.08), 0.06 (0.02,0.11),	**0.02, 1.8e-3**	0.03 (0,0.06), 0.03 (-0.01,0.07),	0.11, 0.18
lFPN	pDMN	4	0.04	0.05 (-0.01,0.11)	0.14	0.07 (0,0.13)	**0.04**	0.03 (-0.04,0.07)	0.79
lFP	aDMN	3, 4	6.1e-4, 1.6e-4	0.03 (-0.02,0.07), 0.09 (0.03,0.14),	0.35, **1.07e-3**	0.07 (0.02,0.12), 0.09 (0.03,0.15),	**5.65e-4, 8.1e-4**	0.04 (0,0.09), 0.01 (-0.05,0.06),	0.13, 0.97
rFPN	aDMN	4	3.61e-6	0.09 (0.04,0.15)	**1.5e-4**	0.11 (0.05,0.16)	**1.5e-5**	0.02 (-0.03,0.07)	0.72

Table 1. p-values of the group variable (p(Group)) that show significant differences in mean ciPLV values for a 1-way ANOVA model are shown. Both MCI and AD patients show significantly reduced ciPLV between the FPN and aDMN networks compared to CN, while only AD patients show a significant reduction between FPN and pDMN compared to CN. These differences are observed primarily in the higher order IMFs (IMF_3 and IMF_4). The significant Scheffe's post hoc p-values at p<0.05 are highlighted in bold.

Figure 4. Results of group wise partial correlation analysis between phase synchronization (ciPLV) and amyloid deposition (SUVR) are shown. CN patients showed a positive association between SUVR and ciPLV (r = 0.29) involving lFPN and aDMN RSNs. However, MCI showed a negative relationship between SUVR and ciPLV (r =-0.19) for rFPN and aDMN. No significant associations were identified in AD patients.